

## Direct Observation of Strain-Induced Change in Surface Electronic Structure

Daiichiro Sekiba,\* Kan Nakatsuji, Yoshihide Yoshimoto, and Fumio Komori

*Institute for Solid State Physics, Kashiwanoha 5-1-5, Kashiwashi, Chiba 277-8581, Japan*

(Received 31 August 2004; published 11 January 2005)

We have observed a novel modification of a surface state due to a local strain field induced by a nanopattern formation. N adsorption on the Cu(100) surface induces a nanoscale grid pattern, where the clean Cu regions remain periodically. The lattice is contracted on the clean region by adjacent  $c(2 \times 2)$ N domains, which have a larger lattice constant. On this patterned surface, we have investigated the Tamm-type surface state at  $\bar{M}$  by means of angle-resolved ultraviolet photoelectron spectroscopy. The binding energy of the Tamm state shifts toward the Fermi level continuously with increasing N coverage, i.e., the intensity of the strain field. This behavior due to the strain field is completely different from that caused by electron confinement observed on vicinal surfaces. The Brillouin zone extension corresponding to the lattice contraction was also detected.

DOI: 10.1103/PhysRevLett.94.016808

PACS numbers: 73.20.At, 73.22.-f

Metal surfaces often show typical surface electronic states such as Shockley or Tamm states. These surface states play an important role in various physical and chemical properties: magnetism in thin film [1], epitaxial growth, and surface chemical reaction, etc. Up to now, a number of studies have been performed to tailor the surface states and give them a novel property. One of the common methods for the tailoring is to use regularly arrayed atomic steps induced by crystal miss cut. Recent experiments have revealed that the steps on the vicinal surfaces can confine the electrons in both the Tamm state at  $\bar{M}$  on Cu(100) [2] and the Shockley state at  $\bar{\Gamma}$  on Cu(111) [3].

In addition to confinement, we can introduce “strain field” caused by a nanopattern formation as a new tool of the surface state tailoring. The electronic structure change due to the strain has been implied by several studies of epitaxial growth [4,5] and molecular adsorption on metal surfaces [6–9]. The strain in the lattice modifies the sticking and dissociation probabilities and the adsorption energy through the change of the electronic states. These will lead to the formation of useful nanostructures and the development of efficient catalysts by controlling the strain. However the strain-induced change of the valence electronic structure has never been directly confirmed by experiments.

In the present Letter, we report the strain-induced modification of the Tamm state at  $\bar{M}$  on the Cu(100) surface being observed by angle-resolved ultraviolet photoelectron spectroscopy (ARUPS). We also show an evidence of the Brillouin zone extension corresponding to the lattice constant reduction. Here, a local strain field of the lattice is induced by nitrogen (N) partial adsorption on the Cu(100) surface. The experimental results will be fully supported by first-principles calculations.

Nitrogen adsorbs on the Cu(100) surface after 500 eV N-ion exposure and annealing at 400 °C for 5 min [10]. The dissociated N atom stays at the four-fold hollow site, and the N-adsorbed area forms a square  $c(2 \times 2)$ N nano-

domain. On the domain, compressive stress is induced by the adsorption, and the dimension of the domain is usually restricted within  $5 \text{ nm} \times 5 \text{ nm}$  at low N coverage to reduce the lattice elastic energy [11]. At 0.3 monolayer (ML) of the averaged N coverage, the surface is covered with a well-ordered array of the N-adsorbed domain, a so called grid surface, as schematically shown in Fig. 1. Here ML is defined as unreconstructed Cu density at the clean surface, and the local density of N at the domain is 0.5 ML. The dark area in Fig. 1 is the N-adsorbed domain, and the white part is a remaining clean Cu region. The clean region is compressed because of the Cu atom displacement on the surrounding N-adsorbed domains [11]. Inhomogeneous atom displacement from the bulk lattice was experimentally observed by STM [12]. In a simple approximation, the

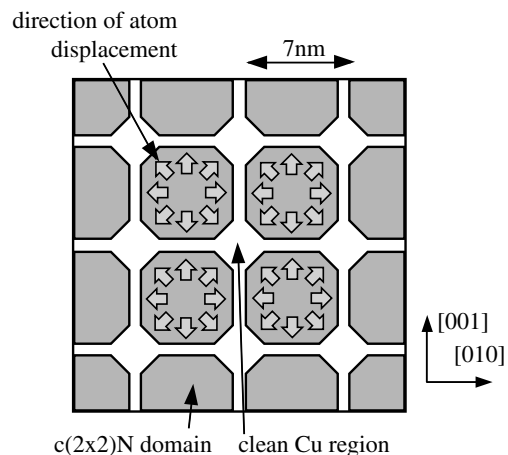


FIG. 1. A schematic illustration of N-induced gridlike nanopattern on the Cu(100) surface. Gray areas indicate the N-adsorbed  $c(2 \times 2)$ N domain, and white area represents the remaining clean Cu region. N adsorption causes displacement of Cu atoms as shown by arrows on the  $c(2 \times 2)$ N domains, so that the clean regions are strongly compressed by surrounding  $c(2 \times 2)$ N domains.

Cu lattice deformation on average will be proportional to the N coverage. We have aimed to detect the Tamm-type surface state on this remaining Cu clean region by ARUPS with changing the N coverage, and to compare the results with those on the clean surface.

A Cu(100) single crystal was cleaned by  $\text{Ar}^+$  ion bombardment and  $600^\circ\text{C}$  annealing cycles. For the grid surface, we always confirmed a sharp  $c(2 \times 2)$  LEED pattern accompanied by four-fold satellite spots, which indicate the formation of the well-ordered super lattice. For ARUPS we used a SCIENTA SES100 analyzer. The sample was kept at 130 K during the measurements. The combination of the HeI radiation (SPECS UVS300) and a triple mirror polarizer was used as an ultraviolet photon (UV) source. The photoelectron was detected in the light incidence plane. ARUPS spectra were taken along the  $\bar{\Gamma} - \bar{M}$  line (the [100] direction). The base pressure of the analyzer chamber was less than  $1 \times 10^{-10}$  Torr.

Figs. 2(a)–2(d) show the experimental band maps around  $\bar{M}$  taken on the clean, 0.1 ML, 0.2 ML, and 0.3 ML N-adsorbed surfaces, respectively. The maps were obtained by taking the second derivative of the ARUPS spectra. Bright parts correspond to the energy bands. On the clean surface, we can clearly see the intense Tamm state symmetrically folding at  $\bar{M}$  ( $k = 1.74 \text{ \AA}^{-1}$ )

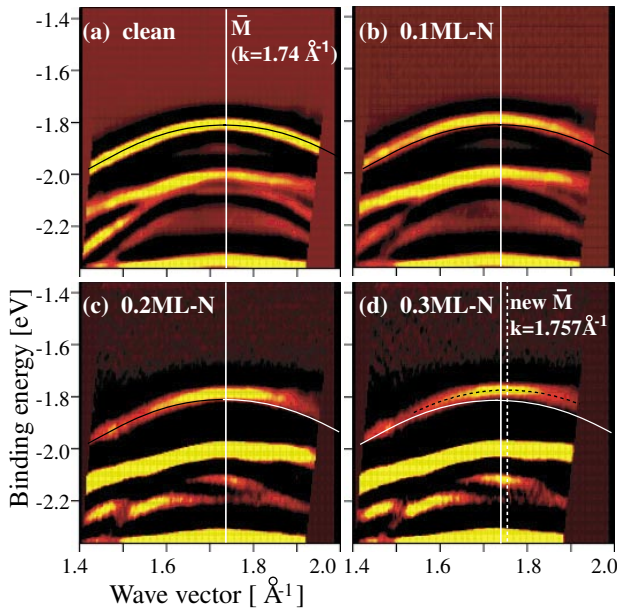


FIG. 2 (color online). Band dispersions experimentally observed on the clean (a), 0.1 ML N-adsorbed (b), 0.2 ML (c), and 0.3 ML (d) surfaces. The solid black (or white) curve in each figure indicates the band dispersion of the Tamm state determined on the clean surface. The dotted curve in (d) shows the Tamm state band dispersion on the grid surface determined by peak analysis and fitting. The white solid line in each figure represents the folding point of the Tamm state on the clean surface, and the white dotted line in (d) shows the new folding point.

with the binding energy (BE) of  $-1.81 \text{ eV}$ . A solid black (or white) curve in each figure indicates the band dispersion of the Tamm state determined on the clean surface. From the data on the N-adsorbed surfaces, we can see two kinds of electronic structure changes: (1) BE of the Tamm state decreases with increasing N coverage, i.e., the increase of the strain at the clean region, (2) the folding point of the Tamm state moves to a larger  $k$  point with increasing the strain.

First, we have to confirm that those changes are really caused by the strain at the clean region, instead of a chemical shift due to the Cu – N bond. Figure 3(a) shows ARUPS spectra at  $\bar{M}$ . The spectra are normalized with the anode current of the UV source. The name on each peak (S4-S6, B2, B3) is referred from a recent report [13]. The notations S and B signify the surface state and the bulk state, respectively. In this figure, an intense peak of the Tamm state (S4) can be seen at  $-1.81 \text{ eV}$  on the clean surface. The intensity of the Tamm state rapidly decreases with increasing the N coverage, and it disappears completely on the 0.4 ML surface, where only very narrow clean regions remain. Now we can conclude that there is no Tamm state on the N-adsorbed domain on the grid surface, because both the grid and the saturated surfaces have the same local N-adsorbed  $c(2 \times 2)$  structure. In other words, the Tamm state is fully consumed by Cu – N bonding on the  $c(2 \times 2)$  N domain. Therefore the surface state peaks at  $\bar{M}$  seen in Fig. 3(a) are the signals only from the remaining clean regions.

Thus it is probable that the electronic structure changes observed in Fig. 2 are caused by the strain. The strain at the

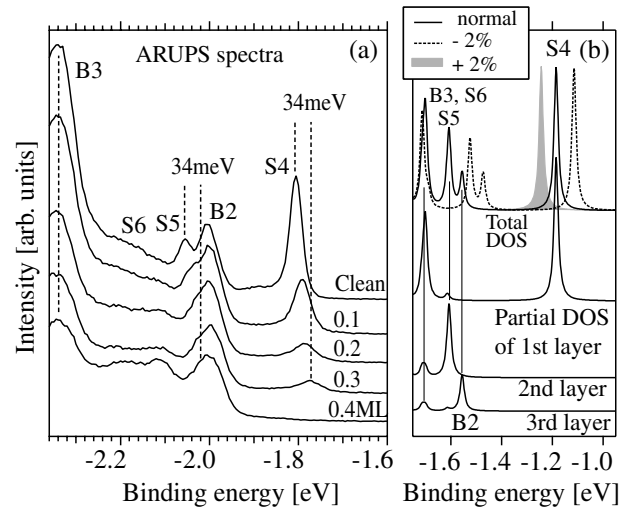


FIG. 3. (a) ARUPS spectra at  $\bar{M}$  on the clean and N-adsorbed (0.1–0.4 ML) Cu(100) surfaces. (b) Calculated DOS of surface and individual atomic layers at  $\bar{M}$ . The top solid (dotted) curve indicates the DOS without (with) 2% lattice constant reduction. The gray peak indicates the Tamm state (S4) for the 2% lattice constant expansion. The peak shifts of S4 and other surface states are clearly predicted. In the lower part of (b), the curves represent the partial DOS of each layer without lattice reduction.

clean region becomes maximum on the grid surface, where the observed Tamm state (S4) shows the BE shift  $\Delta E \sim 34$  meV. Another surface state S5, also shows similar BE and intensity modifications. The peaks of B2 and B3 reduce their intensity, but do not show a significant BE change. As for S6, its intensity is too weak to discuss the peak shift. We can estimate the reduction of the lattice constant on the clean region from the folding point of the Tamm state. By the fitting with the parabolic function [the dotted curve in Fig. 2(d)], the “new”  $\bar{M}$  point is determined as  $k = 1.757 \text{ \AA}^{-1}$  indicating that the lattice constant reduction is  $-1.2\%$ . In detail, the clean region on the grid surface consists of two parts, i.e., narrow lines along [001] and [010] and open spaces at the intersections of the two narrow lines. We note that the above estimated value would be just an average reduction of the lattice constant over the inhomogeneously distorted clean open space region. The contributions from the narrow lines are small and included in the obviously enlarged peak width.

We performed first-principles calculations with a symmetric slab model to discuss the experimental results. The slabs and the vacuum region were 19 and 9 atomic layers thick, respectively. Cu atoms were simulated by ultrasoft pseudopotentials. Standard density-functional plane-wave calculations were carried out using the Perdew-Burke-Ernzerhof (PBE) type exchange-correlation potential [14,15]. The cutoff energy of the plane wave basis set was 81 Ry. All of the symmetry was utilized and the number of the irreducible sampled  $k$  points was  $8 \times (8 + 1)/2 = 36$ . The atomic structures were optimized so that the maximal force acting on an atom became  $3 \times 10^{-4}$  Hartree/a.u. A uniform compressive stress was given to the slabs laterally while interlayer relaxation due to the stress was allowed.

At first, we should assign the peaks in the ARUPS spectra for the clean surface using the calculations, because it has not been successfully done in the precedent study [13]. The ARUPS spectrum at  $\bar{M}$  taken on the clean surface with nonpolarized light [Fig. 4(a), top] is compared with a calculated density of state (DOS) [Fig. 4(b), top]. In the calculation, we used the following assumptions. First, the DOS consists of the Lorentzians possessing 0.01 eV width. Second, the DOS is constructed by the summation of partial DOS of the topmost three layers. Third, the reductive factors for the partial DOS is taken into account for simulating the escape depth of the photoelectrons; 100% of the first, 50% of the second, and 25% of the third. In the experimental spectrum we can see five features B2, B3, S4, S5, and S6, while there are only four distinctive peaks in the calculated DOS. To make clear the assignments, we tried symmetry analysis of each state by using polarized light. The middle and bottom curves in Fig. 4(a) show the ARUPS spectra at  $\bar{M}$  with  $p$  and  $s$  polarization, respectively. Here the degree of the light polarization is 90%. Relatively to the B3 intensity, those of B2, S4, and S5 are

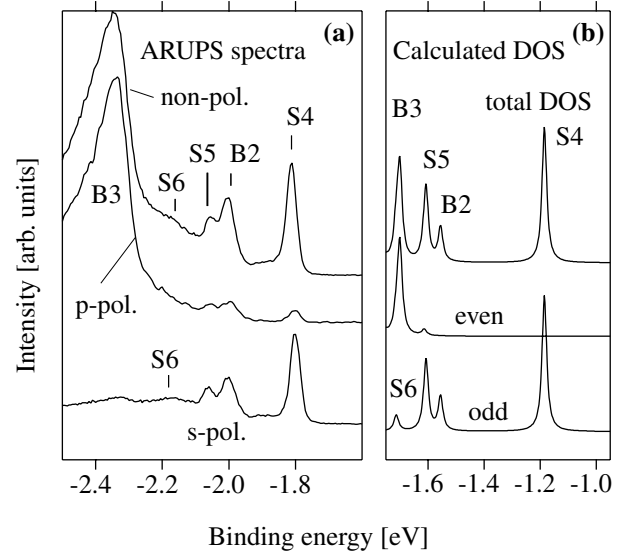


FIG. 4. (a) ARUPS spectra at  $\bar{M}$  taken on the clean surface with nonpolarized (top),  $p$ -polarized (middle), and  $s$ -polarized light (bottom). The names of peaks B2, B3, S4, S5, and S6 are referred from a previous report [13]. (b) Calculated DOS of nonstrained Cu(100) surface. The top spectrum shows the total DOS of the topmost three surface layers (see main text). The even and odd symmetry components of this DOS are also displayed in the middle and the bottom, respectively.

strongly suppressed and S6 is now invisible in the data of  $p$  polarization. Oppositely with the  $s$  polarization, B3 feature is reduced whereas B2, B3, S4, S5, and S6 are clearly seen. From these data, we know that B3 has even symmetry with respect to the  $\bar{\Gamma} - \bar{M}$  line, while B2, S5, S6, and S4 have odd symmetry. On the other hand, the calculated DOS is also resolved into the even and odd components as the middle and bottom curves in Fig. 4(b). In the even component of the DOS, there is a unique distinct peak around  $\sim -1.65$  eV, and we should assign this to B3. A small peak next to B3 in this component may not be visible in the experiments. Four features are observed in the odd component around  $\sim -1.65$  eV,  $\sim -1.60$  eV,  $\sim -1.58$  eV, and  $\sim -1.2$  eV, and it is reasonable to attribute them to S6, S5, B2, and S4, respectively.

Now we discuss how each calculated state assigned above behaves with applied strain field. Figure 3(b) illustrates the DOS change due to the 2% of lattice constant reduction of Cu(100). The DOS without and with the reduction are shown by the solid and dotted curves, respectively, [Fig. 3(b), top]. The same procedure described above was adopted to take into account the photoelectron escape depth. According to these calculated results, the Tamm state S4 ( $\Delta E \sim 67$  meV), and S5 ( $\sim 80$  meV) and B2 ( $\sim 80$  meV) move toward the Fermi level, whereas B3 goes slightly to larger BE. These trends for the surface states are in good agreement with the experimental results except that no energy shift of B2 was observed in the experiment.

The discrepancy for B2, however, is attributed mainly to the inadequate assumption in the present model and the origin of the photoelectrons as follows. First, the strain is strongly localized at the first a few layers on the N-adsorbed Cu(100) surface [11], while in the calculation the compressive stress was uniformly given throughout the slab. Partial DOS of each surface layer is also displayed in Fig. 3(b). According to this, B2 has the maximum partial DOS in the layers deeper than the third layer. In the calculation, the B2 component is also found in the fourth and fifth, and the deeper layers. In such a bulk region, the net strain on the sample from the N-adsorbed domain is much smaller than that of the first layer in the present sample. Second, B2 includes photoelectrons coming from the bulk region below both the clean region and the N-adsorbed domain where the lattice constant is increased. Consequently, B2 may consist of two features: one from the clean region moving slightly toward the Fermi level and the other from the N-adsorbed domain moving slightly to higher BE. In fact, the observed B2 shows just a peak broadening with increasing the N coverage, keeping its peak center at the same position.

We calculated also the electronic structure of the system with a 2% expanded lattice constant to examine our discussion. The result shows a perfect linear response, i.e., S4 ( $\Delta E \sim -60$  meV), S5 ( $\Delta E \sim -50$  meV), and B2 ( $\Delta E \sim -72$  meV) move away from the Fermi level, while B3 stays almost at the same position. Therefore we can conclude that the peak shifts in the calculation are caused by a lattice contraction effect, not by some other artifacts. The state S4 with the 2% expansion is shown in Fig. 3(b) by a gray-colored peak.

Apart from the above peaks, the calculation predicted that a surface state around  $-5$  eV shows a large energy shift  $\Delta E \sim -120$  meV toward deeper BE (not reported here). Unfortunately in our experiment, this BE region is dominated by  $N2p$  states, and we could not observe a distinct energy shift of this state. Its shift due to strain would be seen in an experiment using another way of strain application instead of N adsorption.

As a final point, we compare our results with the previous studies on the Tamm state confined on vicinal surfaces. Two groups performed ARUPS measurements on the Cu(610) surface, where there are regular steps in every six Cu atomic rows [16,17]. In this case, the Tamm state showed the  $\sim -40$  meV BE shift away from the Fermi energy and the band dispersion was reduced. These results were well interpreted by the Kronig-Penney model with negative effective mass [2]. In our case, the BE of the Tamm state shifts  $\sim 34$  meV toward the Fermi level, oppositely to the results on the vicinal surface. Furthermore, the Tamm state in the clean region does not show any explicit reduction of the band dispersion. This indicates that the clean region in the grid surface is not so narrow as the

terrace on the Cu(610) surface, and the confinement effect is insufficient.

In conclusion, we have observed the first direct evidence of the local strain field effect onto the surface states of Cu(100) by means of ARUPS. We induced the local strain field by N adsorption on the surface. The Brillouin zone extension corresponding to the lattice constant reduction was also detected. The experimental results are in excellent agreement with the first-principles calculations for the surface states. We expect that our results will give useful information for the strain-dependent surface processes of atoms such as epitaxial growth and chemical reactions.

We performed the first-principles calculations by an extended version of the program package TAPP [18] on the facilities of the Supercomputer Center, Institute for Solid State Physics, University of Tokyo.

---

\*Electronic address: sekiba@issp.u-tokyo.ac.jp

- [1] L. Diekhoner, M.A. Schneider, A.N. Baranov, V.S. Stepanyuk, P. Bruno, K. Kern, Phys. Rev. Lett. **90**, 236801 (2003).
- [2] A. Beckmann, Ch. Ammer, K. Meinel, and H. Neddermeyer, Surf. Sci. Lett. **432**, L589 (1999).
- [3] F. Baumberger, M. Hengsberger, M. Muntwiler, M. Shi, J. Krempasky, L. Patthey, J. Osterwalder, and T. Greber, Phys. Rev. Lett. **92**, 196805 (2004).
- [4] V.S. Stepanyuk, D.I. Bazhanov, A.N. Baranov, W. Hergert, P.H. Dederichs, J. Kirschner, Phys. Rev. B **62**, 15 398 (2000).
- [5] O.V. Lysenko, V.S. Stepanyuk, W. Hergert, and J. Kirschner, Phys. Rev. Lett. **89**, 126102 (2002).
- [6] M. Gsell, P. Jakob, D. Menzel, Science **280**, 717 (1998).
- [7] M. Mavrikakis, B. Hammer, and J.K. Nørskov, Phys. Rev. Lett. **81**, 2819 (1998).
- [8] Y. Uesugi-Saitow and M. Yata, Phys. Rev. Lett. **88**, 256104 (2002).
- [9] S. Ohno, K. Yagyuu, K. Nakatsuji, and F. Komori, Surf. Sci. **554**, 183 (2004).
- [10] F.M. Leibsle, C.F.J. Flipse, and A.W. Robinson, Phys. Rev. B **47**, 15 865 (1993).
- [11] C. Cohen, H. Ellmer, J.M. Guigner, A. L'Hoir, G. Prévot, D. Schmaus, and M. Sotito, Surf. Sci. **490**, 336 (2001).
- [12] S. Ohno, K. Yagyuu, K. Nakatsuji, and F. Komori, Surf. Sci. Lett. **547**, L871 (2003).
- [13] C. Baldacchini, L. Chiodo, F. Allegretti, C. Mariani, M.G. Betti, P. Monachesi, and R. Del Sole, Phys. Rev. B **68**, 195109 (2003).
- [14] J.P. Perdew, K. Burke, and M. Ernzerhof, Phys. Rev. Lett. **77**, 3865 (1996).
- [15] J.P. Perdew, K. Burke, and M. Ernzerhof, Phys. Rev. Lett. **78**, 1396 (1997).
- [16] R. Matzdorf and A. Goldmann, Surf. Sci. **400**, 329 (1998).
- [17] M. Hengsberger, D. Purdie, M. Garnier, K. Breuer, and Y. Baer, Surf. Sci. **405**, L491 (1998).
- [18] J. Yamauchi, M. Tsukada, S. Watanabe, and Osamu Sugino, Phys. Rev. B **54**, 5586 (1996).